Iterative Design of Concentration Factors for Jump Detection[*]

Adityavikram Viswanathan[†]   Anne Gelb[‡]   Douglas Cochran[§]

August 30, 2011

Abstract

The concentration method of edge detection was developed to compute the locations and values of jump discontinuities in a piecewise-analytic function from its first few Fourier series coefficients. The accuracy and characteristic features of the resulting jump approximation depend on Fourier space "filter" factors known as concentration factors. In this paper, we provide a flexible, iterative framework for the design of these factors. Previously devised concentration factors are shown to be the solutions of specific problem formulations within this new framework. We also provide sample formulations of the procedure applicable to the design of concentration factors for data with missing spectral bands. Several illustrative examples are used to demonstrate the capabilities of the method.

1   Introduction

Detection and characterization of abrupt changes in signals are important in many signal processing applications. A sudden change in the amplitude of a one-dimensional signal often indicates a significant transition in the state of the signal source, such as catastrophic failure of a component in a mechanical or electrical system. Accurate estimation of the time of the leading edge of an emitted radar pulse at multiple distributed receivers provides a means for passive localization of the emitter. In image processing and other multi-dimensional applications, detection of sharp transitions is valuable for segmentation and descriptors of edges and other abrupt phenomena in data are often used as features

in pattern recognition. In the solution of PDEs using spectral methods, identification of jump discontinuities and associated processing can greatly improve the accuracy of the solutions.

In some of these cases, we may be required to identify jumps in the data given measurements in the Fourier domain. This is the case in applications such as magnetic resonance imaging (MRI) and synthetic aperture radar (SAR). The underlying physics of these problems models the signal acquisition process as the collection of samples of the Fourier transform of the specimen being imaged. The detection of jumps from such data is a challenging problem, since Fourier data constitutes a global representation, from which we seek accurate representations of a local phenomenon.

The concentration method of edge detection, [1], was devised with exactly this in mind. It computes an approximation to what is known as the *jump function* (defined in Section 2) from the first $2N + 1$ Fourier series coefficients of the function using a partial Fourier sum and Fourier space "filter" factors known as *concentration factors*. The characteristic properties of the resulting approximation, including the behaviors in the neighborhood of jumps and smooth regions away from jumps, are determined by these factors. In this paper, we present an iterative framework for the design of these factors. Admissible concentration factors are shown to be generated by solving an iterative, and typically convex program. Some of the traditional concentration factors, originally derived in [1,2], are shown to be the solutions of particular problem formulations within our new framework. In addition, this framework admits the design of factors satisfying specific constraints with regard to the resulting jump approximation. We also present the application of this framework to the design of concentration factors with missing or banded spectral data. Unavailability of data in some frequency bands is common in practice due to several causes, including limitations in sensor capability, the presence of strong incidental or intentional narrowband interference, and communication link restrictions or dropouts.

The rest of the paper is organized as follows: Section 2 summarizes the concentration edge detection method, including the notion of a jump function, concentration factors and their admissibility conditions. A few prototypical families of concentration factors are tabulated and their performance on test functions illustrated. The notion of *low* and *high order* edge detectors is also briefly explained. Section 3 starts by providing a summary of previous and related work on the topic, before introducing our new framework of concentration factor design. This section contains several sample problem formulations that illustrate the flexibility of the framework, while also serving to associate some of the traditional concentration factors with specific iterative formulations. Section 4 examines the application of the framework to missing or banded spectral data. We give some concluding comments and avenues for future investigation in Section 5.

2 The Concentration Edge Detection Method

Let f be a 2π-periodic piecewise-smooth function[1] defined in $[-\pi, \pi)$. We will assume that we are given the Fourier series coefficients

$$\hat{f}(k) = \frac{1}{2\pi} \int_{-\pi}^{\pi} f(x)e^{-ikx}dx, \quad k = -N, ..., N. \tag{1}$$

Definition 1. *(Jump Function) Let the right and left-hand limits of the function, $f(x^+)$ and $f(x^-)$, be defined at every point x in the domain. The jump function associated with f and denoted by $[f]$ is defined as the difference between the right and left hand limits of the function at every point x; i.e.,*

$$[f](x) := f(x^+) - f(x^-). \tag{2}$$

Note that the jump function is non-zero only at a jump discontinuity, where it takes the value of the jump.

Given the first $2N + 1$ Fourier coefficients of a piecewise-smooth function, the concentration edge detection method, [1,2], computes an approximation to the jump function using a partial sum of the form

$$S_N^\sigma[f](x) = i \sum_{|k| \le N} \hat{f}(k) \operatorname{sgn}(k) \, \sigma\left(\frac{|k|}{N}\right) e^{ikx}. \tag{3}$$

The convergence properties of the jump approximation depend on the choice of factors $\sigma(\eta) = \sigma\left(\frac{|k|}{N}\right)$, which are known as *concentration factors*. As discussed in [2], these factors satisfy the following admissibility conditions:

1. $\displaystyle\sum_{k=1}^{N} \sigma\left(\frac{k}{N}\right) \sin(kx)$ is odd

2. $\displaystyle\frac{\sigma(\eta)}{\eta} \in C^2(0, 1)$

3. $\displaystyle\int_{\epsilon}^{1} \frac{\sigma(\eta)}{\eta} \to -\pi$, where $\epsilon = \epsilon(N) > 0$ is small.

It is illustrative to note that the equivalent physical-space representation of the concentration sum in (3) is the convolution of f with a *concentration kernel* C_N^σ defined as

$$C_N^\sigma(x) := i \sum_{|k| \le N} \operatorname{sgn}(k)\sigma\left(\frac{|k|}{N}\right) e^{ikx}. \tag{4}$$

---

[1] We restrict our attention to real-valued functions, since practical applications typically demand the identification and characterization of real-valued jumps.

Thus (3) is equivalent to

$$S_N^\sigma[f](x) = (f * C_N^\sigma)(x). \tag{5}$$

The admissibility conditions simply state that this kernel is required to be odd and suitably normalized in order to approximate the jump function. A certain amount of smoothness is also required as embodied in condition 2. If these conditions are satisfied, $S_N^\sigma[f]$ "concentrates" at the singular support of f and the jump approximation obeys the concentration property, [5, Theorem 2.3],

$$S_N^\sigma[f](x) = [f](x) + \begin{cases} \mathcal{O}\left(\frac{\log N}{N}\right) & d(x) \lesssim \frac{\log N}{N} \\ \mathcal{O}\left(\frac{\log N}{(Nd(x))^s}\right) & d(x) \gg \frac{1}{N}. \end{cases} \tag{6}$$

Here, $d(x)$ denotes the distance between a point in the domain and the nearest discontinuity, while $s > 0$ depends on the concentration factor chosen. Use of a *higher-order*[2] edge detector results in a larger value of s as compared to using a *lower-order* edge detector. Table 1 lists a selection of concentration factors introduced in [1, 2], while Figure 1 plots these factors in the Fourier domain.

Factor	Expression	Remarks
Trigonometric	$\sigma_G(\eta) = \dfrac{\pi \sin(\pi\eta)}{\text{Si}(\pi)}$	$\text{Si}(\pi) = \displaystyle\int_0^\pi \frac{\sin(x)}{x}\, dx$
Polynomial	$\sigma_P^p(\eta) = p\pi\eta^p$	p is the order of the factor
Exponential	$\sigma_E(\eta) = C\,\eta\, e^{\left(\frac{1}{\alpha\eta(\eta-1)}\right)}$	α is the order C is a normalizing constant $C = \dfrac{\pi}{\int_{\frac{1}{N}}^{1-\frac{1}{N}} \exp\left(\frac{1}{\alpha\tau(\tau-1)}\right) d\tau}$

Table 1: Examples of concentration factors

Each concentration factor generates a unique oscillatory response in the immediate vicinity and away from jumps. We will refer to this as the *jump response* associated with a concentration factor.

Let $\sigma(\eta)$ be an admissible concentration factor. Let $r(x)$ denote the unit ramp function, with a corresponding jump function $[r](x)$.

$$r(x) = \begin{cases} \frac{-x-\pi}{2\pi} & x < 0 \\ \frac{\pi-x}{2\pi} & x > 0 \end{cases}, \qquad [r](x) = \begin{cases} 1 & x = 0 \\ 0 & \text{else}. \end{cases}$$

Definition 2. *(Jump Response) The jump response associated with a concentration factor σ, denoted by $W_0^{\sigma,N}(x)$, is defined as the jump function approxi-*

---

[2]The notion of low and high order edge detectors and their characteristic features will be discussed below.

4
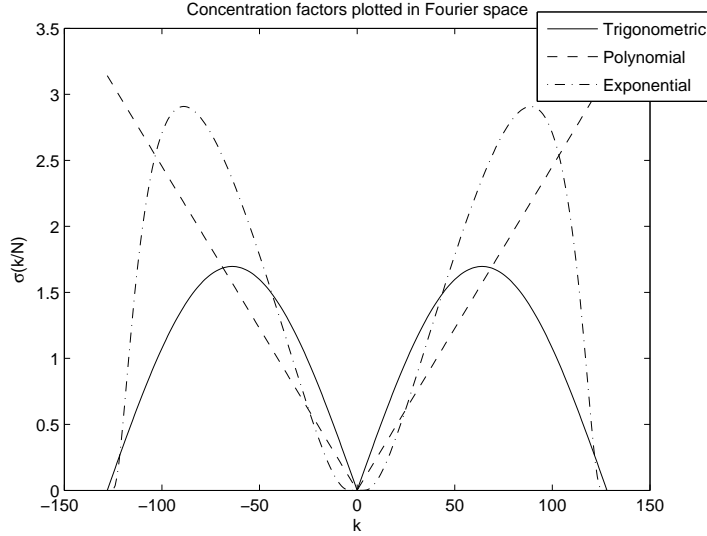
Figure 1: Concentration factors plotted in Fourier space, $N = 128$

mation of the unit ramp as generated by the concentration sum (3). i.e.,

$$W_0^{\sigma,N}(x) := S_N^\sigma[r](x) = i \sum_{|k| \leq N} \hat{r}(k)\, sgn(k)\, \sigma\left(\frac{|k|}{N}\right) e^{ikx}$$

$$= \frac{1}{2\pi} \sum_{0 < |k| \leq N} \frac{\sigma\left(\frac{|k|}{N}\right)}{|k|} e^{ikx}. \qquad (7)$$

The final equation is obtained by substituting the Fourier coefficients of the ramp function,

$$\hat{r}(k) = \begin{cases} \frac{1}{2\pi i k} & k \neq 0 \\ 0 & k = 0. \end{cases}$$

The jump responses of each of the concentration factors listed in Table 1 are plotted in Figure 2. These plots serve to illustrate the "concentration" of the jump approximation at the jump location. Note also the non-uniform convergence to the true jump function, as stated in (6). The different orders of convergence away from the jump for each of the concentration factors, parameterized by s in (6), is also seen from the plots. For example, the polynomial concentration factor shows slowly decaying oscillations for $|x| > 0$, while the exponential factor shows a vanishing response away from the jump.

As evidence of the use of this method on more general functions, consider the jump approximations of the two test functions in (8) and (10), plotted in
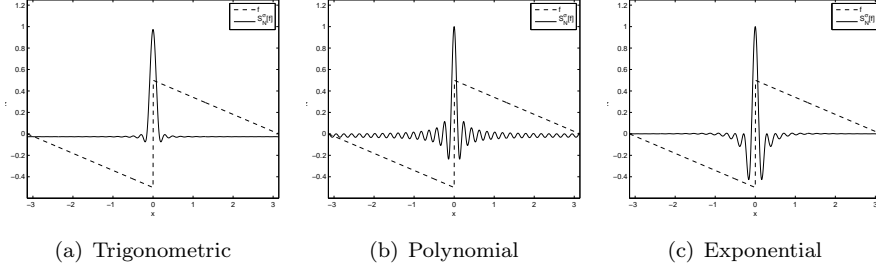
5

(a) Trigonometric   (b) Polynomial   (c) Exponential

Figure 2: Characteristic responses of different concentration factors to a ramp function $(N = 32)$

Figure 3 (a) and (b) respectively. The true jump functions are provided for reference in (9) and (11) respectively.

$$f_1(x) = \begin{cases} \frac{3}{2} & -\frac{3\pi}{4} \le x < -\frac{\pi}{2} \\ \frac{7}{4} - \frac{x}{2} + \sin(x - \frac{1}{4}) & -\frac{\pi}{4} \le x < \frac{\pi}{8} \\ \frac{11}{4}x - 5 & \frac{3\pi}{8} \le x < \frac{3\pi}{4} \\ 0 & \text{else.} \end{cases} \tag{8}$$

$$[f_1](x) = \begin{cases} \frac{3}{2} & x = -\frac{3\pi}{4} \\ -\frac{3}{2} & x = -\frac{\pi}{2} \\ \frac{14+\pi}{8} - \sin\left(\frac{\pi+1}{4}\right) \approx 1.28 & x = -\frac{\pi}{4} \\ \sin\left(\frac{2-\pi}{8}\right) - \frac{28-\pi}{16} \approx -1.70 & x = \frac{\pi}{8} \\ \frac{33\pi}{32} - 5 \approx -1.76 & x = \frac{3\pi}{8} \\ 5 - \frac{33\pi}{16} \approx -1.48 & x = \frac{3\pi}{4} \\ 0 & \text{elsewhere.} \end{cases} \tag{9}$$

$$f_2(x) = \begin{cases} \sin(6x) & -\frac{5\pi}{6} \le x < 0 \\ \frac{1}{\pi}e^{-2x}(\pi - x) & x \ge 0 \\ 0 & x < -\frac{5\pi}{6}. \end{cases} \tag{10}$$

$$[f_2](x) = \begin{cases} 1 & x = 0 \\ 0 & \text{else.} \end{cases} \tag{11}$$

The jump function approximation of $f_1(x)$ was generated using the trigonometric factor while the trigonometric and exponential jump function approximations of $f_2(x)$ are plotted. Note that the trigonometric jump function approximation of $f_2(x)$ has a significant non-zero value in the smooth interval $(-\pi, 0)$. This is an example of a *low-order* edge detector acting on a function with large

6

variation. In comparison, the response using the exponential (*high-order*) factor contains minimal spurious responses in smooth regions[3] at the expense of some additional oscillatory behavior in the immediate vicinity of a discontinuity. Moreover, since the function has significant variation, a larger number of Fourier modes ($N = 100$) are necessary to recover a well resolved jump function approximation.
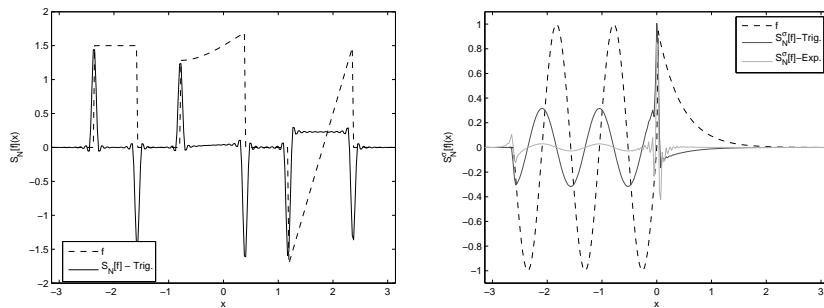
(a) Jump approximation of $f_1(x), N = 64$ (b) Jump approximation of $f_2(x), N = 100$

Figure 3: Jump approximations of two test functions

3   Concentration Factor Design

We start this section by providing a brief summary of previous and related work on this topic. Since the initial development of the concentration edge detection method in $[1, 2]$, several works have addressed the improvement in the resolution of jump approximations. A survey of related literature reveals two broad approaches – enhancements and reformulations of the concentration method itself, and design of new families of concentration factors. Enhancements to the concentration method include nonlinear post-processing procedures such as enhancement of scales, $[2]$, which separates regions (or scales) of jumps from regions of smoothness by raising the jump approximation to a power. As indicated previously and plotted in Figs. 2 and 3, the different concentration factors are characterized by their behavior in the vicinity of a jump and in smooth regions. Use of a multitude of jump responses in conjunction with the *minmod* operator is treated in $[3]$. This results in fewer oscillations near a jump as well as removal of spurious responses in smooth regions. Iterative formulations of the concentration method with connections to the recently developed theory of compressive sensing, $[8, 9]$ were introduced in $[7]$. Here, pre-existing families of concentration factors were utilized in sparsity-enforcing formulations of the concentration method to yield accurate approximations to the jump function. This

---

[3]The small non-zero oscillatory response in the vicinity of $x = -\frac{5\pi}{6}$ is due to a discontinuity in the derivative of $f_2(x)$.

method also allows for the detection of edges from highly incomplete Fourier measurements.

Select literature on the design of new concentration factors can also be found. For example, a family of concentration factors known as matching waveform concentration factors was developed in [4]. These look for correlations in the concentration jump approximation with the jump response of the concentration factor, and results in approximations with reduced oscillatory behavior. The design of concentration factors for noisy data is treated in [5]. The approach in [5] is based on separating the Fourier data into scales of "smoothness", noise and the jump discontinuity. An alternate approach to reducing the effects of noise in concentration edge detection and reconstruction is explained in [6]. We note that each of these works describes the design of a single family of concentration factors. Our present work, in comparison, is more general in formulation and allows for the realization of multiple families of concentration factors.

We start our discussion of concentration factor design by obtaining an expression relating the jump function to the concentration jump response. Consider a periodic function on $[-\pi, \pi)$ with a single jump at $x = \zeta$. We remark that this discussion may be easily generalized to the case of multiple jumps, as long as any two jumps are separated by a distance greater than $\mathcal{O}\left(\frac{\log N}{N}\right)$. We start by expressing the Fourier coefficients in terms of the jump locations and values. For $k \neq 0$, we have

$$\hat{f}(k) = \frac{1}{2\pi} \int_{-\pi}^{\zeta^-} f(x)e^{-ikx}dx + \frac{1}{2\pi} \int_{\zeta^+}^{\pi} f(x)e^{-ikx}dx. \qquad (12)$$

On integrating by parts, we obtain

$$\hat{f}(k) = \left(f(\zeta^+) - f(\zeta^-)\right)\frac{e^{-ik\zeta}}{2\pi ik} + \frac{1}{ik} \cdot \left(\frac{1}{2\pi}\int_{-\pi}^{\zeta^-} f'(x)e^{-ikx} + \frac{1}{2\pi}\int_{\zeta^+}^{\pi} f'(x)e^{-ikx}\right), \qquad (13)$$

where we have used the periodicity of f. From (2), we obtain

$$\hat{f}(k) = [f](\zeta)\frac{e^{-ik\zeta}}{2\pi ik} + \frac{1}{ik} \cdot \left(\frac{1}{2\pi}\int_{-\pi}^{\zeta^-} f'(x)e^{-ikx} + \frac{1}{2\pi}\int_{\zeta^+}^{\pi} f'(x)e^{-ikx}\right).$$

Note that the term within parenthesis is the same as Eq. (12) for f'. Therefore, by repeated integration by parts we obtain

$$\hat{f}(k) = \frac{1}{2\pi}\left(\frac{[f](\zeta)}{ik} + \frac{[f'](\zeta)}{(ik)^2} + \frac{[f''](\zeta)}{(ik)^3} + ...\right)e^{-ik\zeta}, \quad k \neq 0. \qquad (14)$$

Let us now substitute this in the expression for the concentration sum in (3).

$$S_N^\sigma[f](x) = \sum_{0<|k|\leq N} \hat{f}(k) i\sigma\left(\frac{|k|}{N}\right) \text{sgn}(k) e^{ikx}$$

$$= \sum_{0<|k|\leq N} \left[\frac{1}{2\pi}\left(\frac{[f](\zeta)}{ik} + \frac{[f'](\zeta)}{(ik)^2} + ...\right) e^{-ik\zeta}\right] i\sigma\left(\frac{|k|}{N}\right) \text{sgn}(k) e^{ikx}$$

$$= \frac{[f](\zeta)}{2\pi} \sum_{0<|k|\leq N} \frac{\sigma\left(\frac{|k|}{N}\right) \text{sgn}(k)}{k} e^{ik(x-\zeta)}$$

$$+ \frac{[f'](\zeta)}{2\pi} \sum_{0<|k|\leq N} \frac{\sigma\left(\frac{|k|}{N}\right) \text{sgn}(k)}{ik^2} e^{ik(x-\zeta)}$$

$$+ \frac{[f''](\zeta)}{2\pi} \sum_{0<|k|\leq N} \frac{\sigma\left(\frac{|k|}{N}\right) \text{sgn}(k)}{i^2 k^3} e^{ik(x-\zeta)} + ... \quad (15)$$

Recall that the first term in the above equation is a shifted and scaled jump response, $W_0^{\sigma,N}$, (Def. 2). Similarly we may define

$$\frac{1}{2\pi} \sum_{0<|k|\leq N} \frac{\sigma\left(\frac{|k|}{N}\right) \text{sgn}(k)}{ik^2} e^{ikx} := W_1^{\sigma,N}(x), \quad (16)$$

and, in general,

$$\frac{1}{2\pi} \sum_{0<|k|\leq N} \frac{\sigma\left(\frac{|k|}{N}\right) \text{sgn}(k)}{i^q k^{q+1}} e^{ikx} := W_q^{\sigma,N}(x). \quad (17)$$

Substituting in (15), we obtain

$$S_N^\sigma[f](x) = [f](\zeta) W_0^{\sigma,N}(x-\zeta) + [f'](\zeta) W_1^{\sigma,N}(x-\zeta) + [f''](\zeta) W_2^{\sigma,N}(x-\zeta) + ... \quad (18)$$

We note that the jump function is supported on a set of zero measure, making the theoretical development and analysis of the method difficult. To overcome this, we follow [5] and similarly use a regularized equivalent of the jump function, which we denote by $[f]_\epsilon(x)$, and define as

$$[f]_\epsilon(x) = \begin{cases} [f](\zeta) & |x-\zeta| \leq \epsilon, \, \epsilon > 0, \epsilon \sim \mathcal{O}\left(\frac{2\pi}{2N+1}\right) \\ 0 & \text{else.} \end{cases} \quad (19)$$

Thus, (18) becomes

$$S_N^\sigma[f](x) \approx [f]_\epsilon(\zeta)W_0^{\sigma,N}(x-\zeta) + [f']_\epsilon(\zeta)W_1^{\sigma,N}(x-\zeta)+$$
$$[f'']_\epsilon(\zeta)W_2^{\sigma,N}(x-\zeta) + ...$$
$$\approx \int_{-\pi}^{\pi}[f]_\epsilon(\zeta)W_0^{\sigma,N}(x-\zeta)d\zeta + \int_{-\pi}^{\pi}[f']_\epsilon(\zeta)W_1^{\sigma,N}(x-\zeta)d\zeta+$$
$$\int_{-\pi}^{\pi}[f'']_\epsilon(\zeta)W_2^{\sigma,N}(x-\zeta)d\zeta + ...$$
$$= ([f]_\epsilon * W_0^{\sigma,N})(x) + ([f']_\epsilon * W_1^{\sigma,N})(x) + ([f'']_\epsilon * W_2^{\sigma,N})(x) + ... \tag{20}$$

From (16) and (17), we note that $W_i^{\sigma,N}(x) = (\tilde{B}_i * C_N^\sigma)(x)$, where $\tilde{B}_i(x)$ are normalized Bernoulli polynomials[4], [13], and $C_N^\sigma(x)$ is the concentration kernel (4). Since $\tilde{B}_i(x)$ has a discontinuity in its ith derivative at $x = 0$, each of these kernels denotes the response of the concentration sum to jumps in the ith derivative of the function. Since we are interested in identifying jumps, we will call $W_0^{\sigma,N}$ as the jump response of the concentration method to a unit jump or the "jump waveform". The jump response and the first three higher-order kernels associated with the polynomial concentration factor are plotted for illustrative purposes in Figure 4. Note the alternating even-odd nature of the kernels and the reduced scale of the higher order kernel plots.

3.1 Framework for Concentration Factor Design

From the prior discussion, it is clear that the objective in concentration factor design is to emphasize $W_0^{\sigma,N}(x)$, while suppressing the impact of $W_i^{\sigma,N}(x), i > 0$[5]. Further, for a faithful jump approximation, we require (from Def. 1) that $W_0^{\sigma,N}(x)$ have properties similar to the indicator function

$$\delta(x) = \begin{cases} 1 & x = 0 \\ 0 & \text{else.} \end{cases} \tag{21}$$

Consequently, the design framework consists of solving an iterative program which computes a concentration factor σ for (3) such that the above conditions are satisfied. A typical problem formulation takes the form

$$\min_\sigma \quad \phi_0(\sigma)$$
$$\text{subject to} \quad \phi_m(\sigma) = c_m, \quad m = 1, ..., M$$
$$\psi_n(\sigma) \leq d_n, \quad n = 1, ... N. \tag{22}$$

---

[4]High-resolution reconstruction methods for discontinuous data based on subtracting out these Bernoulli polynomials have been pursued successfully in [13].

[5]The necessity to suppress $W_i^{\sigma,N}(x), i > 0$ is evident in the jump function approximation of $f_2(x)$, plotted in Figure 3(b).

(a) Jump response, $W_0^{\sigma,N}(x)$

(b) Kernel $W_1^{\sigma,N}(x)$

(c) Kernel $W_2^{\sigma,N}(x)$
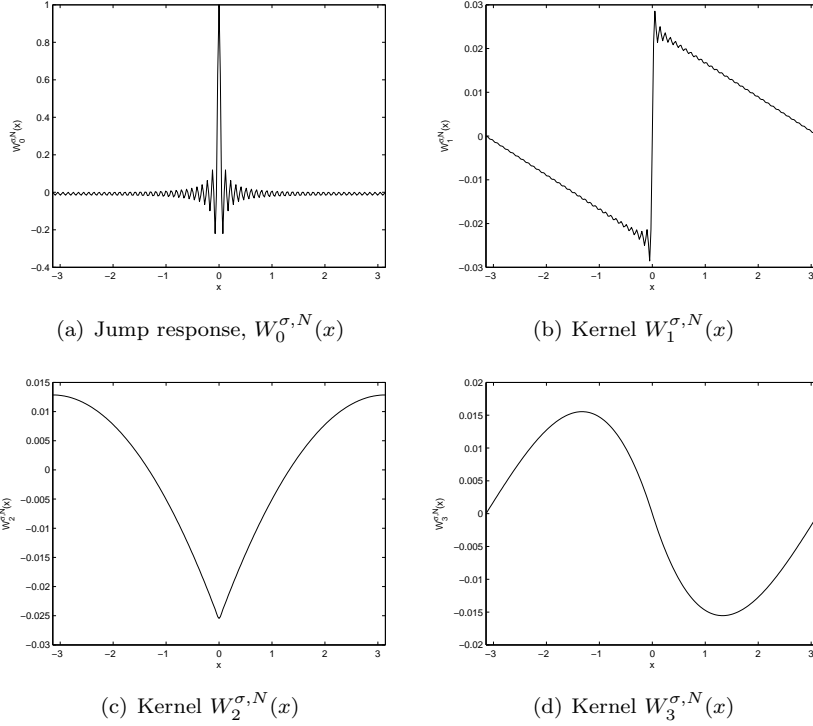
(d) Kernel $W_3^{\sigma,N}(x)$

Figure 4: The jump response and first three higher order kernels associated with the polynomial concentration factor $(N = 64)$

The objective function ϕ_0 is typically a norm measure of $W_0^{\sigma,N}(x)$. In this expression, c_m and d_n are constants or functions independent of σ while the constraints are typically functions of $W_i^{\sigma,N}(x)$ or σ. Sample problem formulations are discussed in Section 3.2. The computational complexity of the problem can be reduced by noting that σ is an even function. This follows from the admissibility condition requiring the concentration kernel (4) to be odd. Consequently, the design problem is an iterative program of size N rather than $2N + 1$.

All problem formulations which are discussed below are convex programs. Most are linear programs or quadratic programs with linear equalities and inequalities. In broad brush, they can all be formulated as second order cone programs (SOCPs), which can be solved using a variety of methods, [10]. In rare cases, problem formulations can lead to quasiconvex problems, which may necessitate other solution methods. In all simulations in this paper, we used CVX, a package for specifying and solving convex programs [11, 12]. Programs were implemented in Matlab (version 7.7) with CVX version 1.2 (build 711).

3.2 Sample Problem Formulations

The following problem formulations serve to illustrate the design framework.

1. Problem Formulation 1 - *The (first-order) polynomial concentration factor*
   We start with a problem formulation minimizing the 2-norm of the jump
   waveform $W_0^{\sigma,N}(x)$, while ensuring it is properly normalized.

$$\min_{\sigma} \quad \| W_0^{\sigma,N} \|_2$$

$$\text{subject to} \quad W_0^{\sigma,N}\Big|_{x=0} = 1. \tag{23}$$

This results in a concentration factor and jump response as plotted in
Figure 5.

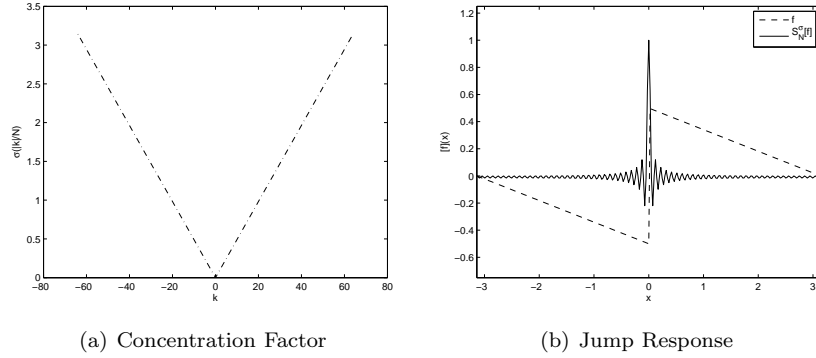(a) Concentration Factor   (b) Jump Response

Figure 5: Problem Formulation 1, $N = 64$

By comparing Figure 5 with Figs. 1 and 2, it is clear that this problem formula-
tion results in the first-order polynomial concentration factor. This conjecture
may be formalized in the following theorem:

Theorem 3.1. *Let $W_0^{\sigma,N}$ be the jump response. The concentration factor
$\sigma(\eta) = \sigma\left(\frac{|k|}{N}\right)$ that solves the problem*

$$\min_{\sigma} \quad \| W_0^{\sigma,N} \|_2$$

$$\textit{subject to} \quad W_0^{\sigma,N}\Big|_{x=0} = 1 \tag{24}$$

is the first-order polynomial concentration factor, $\sigma_P^1(\eta) = \pi\eta$.

Proof. By Parseval's relation, we have

$$\left\| W_0^{\sigma,N} \right\|_2 = \left(\sum_{0<|k|\leq N} \left| \frac{\sigma\left(\frac{|k|}{N}\right)\operatorname{sgn}(k)}{k} \right|^2 \right)^{\frac{1}{2}}$$

$$= \left(\sum_{0<|k|\leq N} \left| \frac{\sigma\left(\frac{|k|}{N}\right)}{|k|} \right|^2 \right)^{\frac{1}{2}}. \tag{25}$$

By defining $\eta = \frac{|k|}{N}$, the above expression becomes

$$\left\| W_0^{\sigma,N} \right\|_2 = \frac{1}{N} \left(\sum_{0<\eta\leq 1} \left| \frac{\sigma(\eta)}{\eta} \right|^2 \right)^{\frac{1}{2}}. \tag{26}$$

The error is minimized when each term in the sum is minimized. Setting $\dfrac{d\left(\frac{\sigma(\eta)}{\eta}\right)^2}{d\eta}$ to zero, we obtain

$$2\left(\frac{\sigma(\eta)}{\eta} \right) \cdot \left(\frac{\eta\sigma'(\eta) - \sigma(\eta)}{\eta^2} \right) = 0.$$

Since $\eta \neq 0$, we have

$$\eta\sigma'(\eta) = \sigma(\eta).$$

The solution of this equation takes the form

$$\sigma(\eta) = C \cdot \eta, \tag{27}$$

where C is some constant. We determine C using the equality constraint, $W_0^{\sigma,N}\big|_{x=0} = 1$.

$$\frac{1}{2\pi} \sum_{0<|k|\leq N} \frac{\sigma\left(\frac{|k|}{N}\right)\operatorname{sgn}(k)}{k} = 1$$

$$\frac{1}{\pi N} \sum_{\eta=1/N}^{1} \frac{\sigma(\eta)}{\eta} = 1$$

$$\frac{C}{\pi N} \cdot N = 1$$

$$C = \pi. \tag{28}$$

The result follows. $\qquad\square$

2. Problem Formulation 2 - *Sparse jump response*
   The jump response of the polynomial concentration factor shows the presence of strong oscillatory behavior in the smooth regions away from the jumps. This can present a significant problem in identification of jumps by thresholding, leading to numerous false positives. We therefore consider a problem formulation where we minimize the 1-norm of the jump waveform $W_0^{\sigma,N}(x)$, subject to the usual normalization constraint.

$$\min_{\sigma} \quad \| W_0^{\sigma,N} \|_1$$

$$\text{subject to} \quad W_0^{\sigma,N}\Big|_{x=0} = 1. \tag{29}$$

This results in a concentration factor and jump response as plotted in Figure 6.

pics

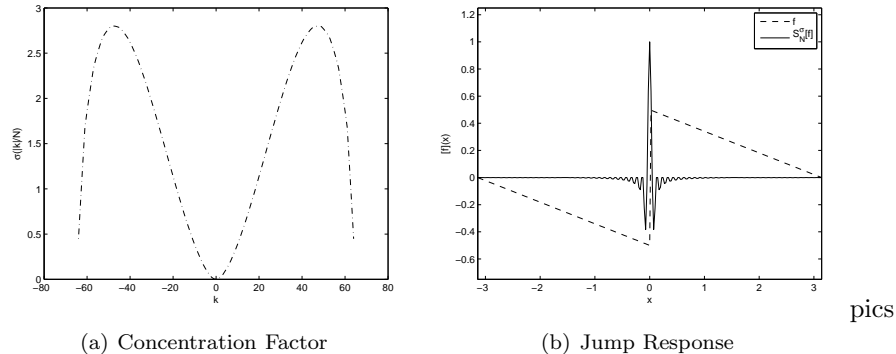(a) Concentration Factor   (b) Jump Response

Figure 6: Problem Formulation 2, $N = 64$

As expected, the response in smooth regions is much smaller. The trade-off, however, is a decreased resolution of the actual jump and strong oscillatory sidelobes in the immediate vicinity of the jump. These features are illustrated in the plots of Figure 7, which plots the absolute error between the true jump function and the concentration jump response on a logarithmic scale. The error plots for different values of N are provided to infer convergence behavior. The almost flat error profile away from the jump in Figure 7(a) (Problem formulation 1) is a result of the slowly decaying oscillations. This is to be contrasted with the vanishing response in the same region in Figure 7(b) (Problem formulation 2).

3. Problem Formulation 3 - *Higher order concentration factors*
   The previous problem formulations impose no constraints on the magnitude of the higher order kernels. From (20), we observe that this can present a problem when computing jump approximations for functions with significant variation and/or with jumps in higher-order derivatives.

14

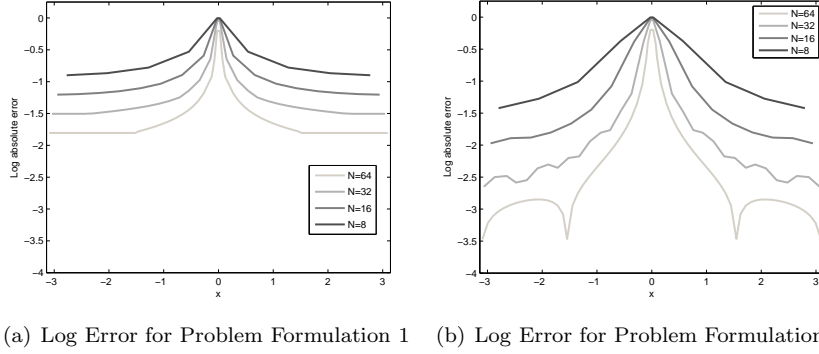(a) Log Error for Problem Formulation 1   (b) Log Error for Problem Formulation 2

Figure 7: Log absolute error between the true jump function and the concentration jump approximation, $N = 64$

This was illustrated in Figure 3 (b), where the jump function approximations of $f_2(x)$ using the (low-order) trigonometric and (high-order) exponential concentration factors were plotted. For reference, we plot in Figure 8 the first four higher-order kernels, $W_i^{\sigma,N}, i = 1, .., 4$, for the trigonometric and exponential concentration factors respectively. Note the logarithmic scale and the significantly reduced values of the kernels for the exponential concentration factor.
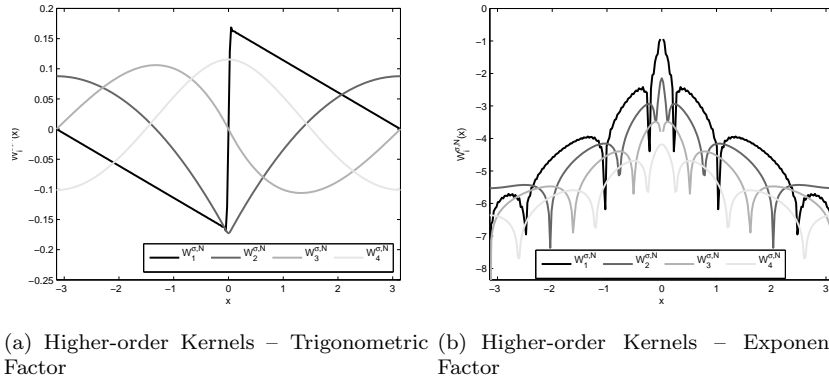

(a) Higher-order Kernels – Trigonometric Factor   (b) Higher-order Kernels – Exponential Factor

Figure 8: Plot of the higher-order kernels, $W_i^{\sigma,N}, i = 1, .., 4$, $(N = 64)$

With this in mind, we consider a problem formulation where we impose

constraints on the higher-order kernels[6].

$$\min_{\sigma} \quad \| W_0^{\sigma,N} \|_1$$

$$\text{subject to} \quad W_0^{\sigma,N} \Big|_{x=0} = 1$$

$$\left\| W_1^{\sigma,N} \right\|_{\infty} \leq 10^{-1}$$

$$\left\| W_2^{\sigma,N} \right\|_{\infty} \leq 10^{-3}$$

$$\sigma \geq 0, \ \sigma(1) = 0. \tag{30}$$

This results in a concentration factor and jump response as plotted in Figure 9.

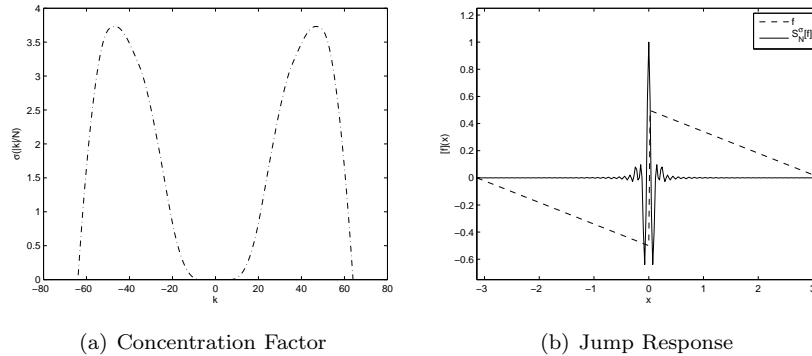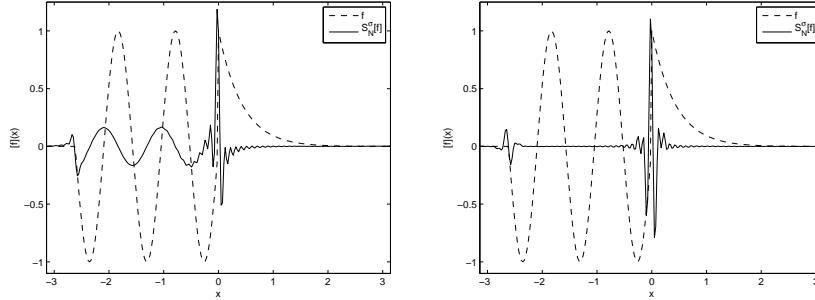(a) Concentration Factor   (b) Jump Response

Figure 9: Problem Formulation 3, $N = 64$

Its effectiveness in canceling out gradients and oscillations is illustrated in Figure 10, which plots the response of the factors from problem formulations 2 and 3 respectively to the test function $f_2(x)$ defined in (10). Problem formulation 2 had no constraints on the higher order kernels; consequently, the jump response in Figure 10 (a) shows a significant non-zero value in the sinusoidal region. In contrast, this part of the jump response in Figure 10 (b) is near zero[7]. Such a concentration factor may be necessary in applications where functions with large variation are encountered, such as the solution of PDEs by spectral methods involving highly oscillatory solutions. Plots of the first four higher-order kernels corresponding to the two concentration factors are given in Figure 11. Note the significantly smaller values for problem formulation 3. It is also illustrative to compare the performance of the factor from problem formulation 3 to the

---

[6]Ideally, the higher-order kernels should be vanishingly small. Programming constraints, however, make this difficult to achieve.

[7]As before, the small oscillatory response in the vicinity of $x = -\frac{5\pi}{6}$ is due to the discontinuities in the derivative and higher-order derivatives of $f_2(x)$.

(a) Jump Approximation – Problem formu-
lation 2 (Low order factor)

(b) Jump Approximation – Problem formu-
lation 3 (High order factor)

Figure 10: Comparison of low and high-order concentration jump approxima-
tions, $N = 64$

exponential concentration factor. The jump function approximations using the
two factors are plotted in Figure 3 (b) and Figure 10 (b) respectively, while
the plots of the higher-order kernels are provided in Figure 8 (b) and Figure
11 (b) respectively. We see that the concentration factor from the iterative
formulation is more effective in canceling out the oscillatory response in the
sinusoidal region. The underlying principle in the design of the two factors, is
however, similar. The exponential factor was designed to cancel out as many
moments as the order of the factor, [2]. Problem formulation 3 serves the same
purpose by canceling out several higher-order kernels. It is conceivable that
a judicious choice of constraints in the iterative program will yield a solution
numerically equivalent to the exponential concentration factor.
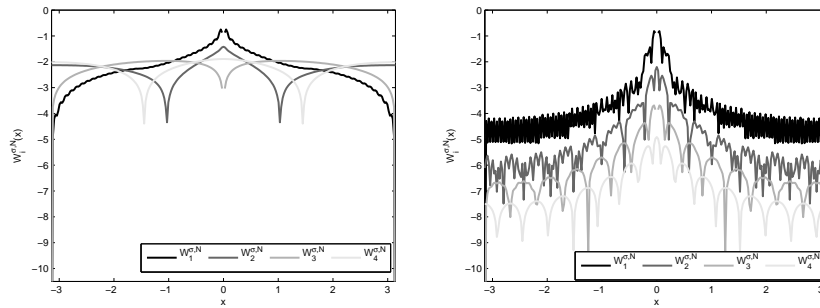
(a) Higher-order Kernels – Problem Formu-
lation 2

(b) Higher-order Kernels – Problem Formu-
lation 3

Figure 11: Logarithmic plot of the higher-order kernels, $W_i^{\sigma,N}, i = 1, .., 4, (N = 64)$

17

4. Problem Formulation 4

The method is also amenable to the imposition of other constraints. As an example, consider the following problem formulation, where we constrain the jump response to be small $(\mathcal{O}(10^{-4}))$ beyond the immediate vicinity of the jump.

$$\min_{\sigma} \quad \| W_0^{\sigma,N} \|_2$$
$$\text{subject to} \quad W_0^{\sigma,N}\Big|_{x=0} = 1$$
$$\left| W_0^{\sigma,N} \right|_{|x|\geq 0.2} \leq 10^{-4}. \tag{31}$$

This results in a concentration factor and jump response as plotted in Figure 12. Note the clean jump response, with just one dominant sidelobe in the immediate vicinity of the jump.
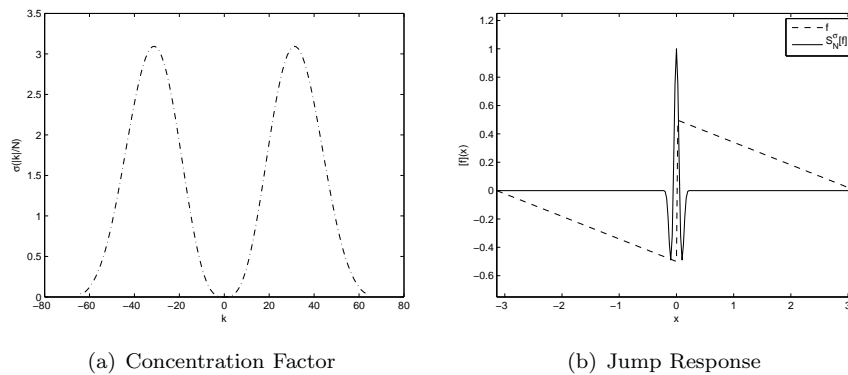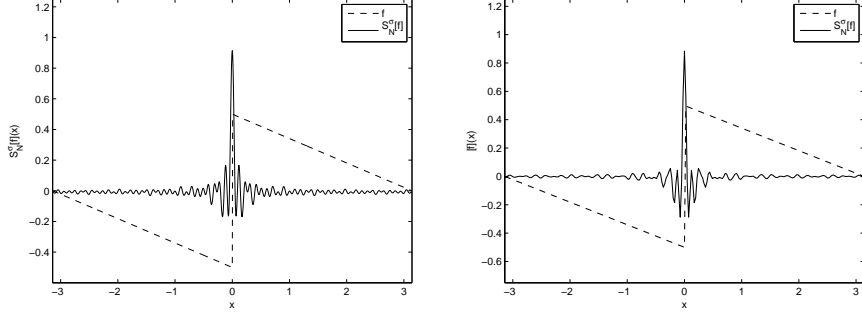

(a) Concentration Factor   (b) Jump Response

Figure 12: Problem Formulation 4, $N = 64$

4 Concentration Factor Design for Missing or Banded Spectral Data

This framework may also be utilized for the design of concentration factors with data missing certain coefficients. In particular, we will look into the problem of data missing measurements in spectral bands. This may be the case due to incidental or intentional narrowband interference, instrumentation errors or unreliable measurements in these bands. The use of standard concentration factors in these cases results in additional spurious oscillations throughout the reconstruction interval, as illustrated in Figure 13. This figure plots the jump response to a unit ramp using the polynomial factor and the concentration factor designed in problem formulation 2. With $N = 64$, Fourier modes $\mathbb{K} = \{k \, | \, 30 \leq |k| \leq 40\}$ are assumed missing.

(a) Jump Response – Polynomial Factor   (b) Jump Response – Problem Formulation 2

Figure 13: Use of standard concentration factors with missing data, $N = 64$

These additional spurious responses can lead to false jump detects, especially in the presence of noise. Hence, we use the design framework to explicitly specify the missing data as a constraint in the problem formulation, as in the following iterative program:

$$
\begin{aligned}
\min_{\sigma} \quad & \| W_0^{\sigma,N} \|_1 \\
\text{subject to} \quad & W_0^{\sigma,N}\Big|_{x=0} = 1 \\
& \sigma(\mathbb{K}) = 0 \\
& \left| W_0^{\sigma,N} \right|_{|x|\geq 0.35} \leq 10^{-3}.
\end{aligned}
\tag{32}
$$

This results in a concentration factor and jump response as plotted in Figure 14. Note the significantly reduced spurious oscillations away from the jump. The one consequence of the missing data, however, is the slightly reduced resolution of the jump itself. Also note that the iterative program implicitly imposes a degree of smoothness in the concentration factor in Fourier space.

Figure 15 plots the performance of the factor on the following test function.

$$
f_3(x) = \begin{cases}
\sin(x) & -\pi \leq x < -\frac{\pi}{2} \\
-\cos\left(\frac{3x}{2}\right) & -\frac{\pi}{2} < x < \frac{\pi}{4} \\
\pi - x & \frac{\pi}{4} < x \leq \pi.
\end{cases}
\tag{33}
$$

$$
[f]_3(x) = \begin{cases}
\frac{\sqrt{2}+1}{\sqrt{2}} \approx 1.707 & x = -\frac{\pi}{2} \\
\frac{3\pi}{4} + \frac{1}{2}\sqrt{2 - \sqrt{2}} \approx 2.734 & x = \frac{\pi}{4} \\
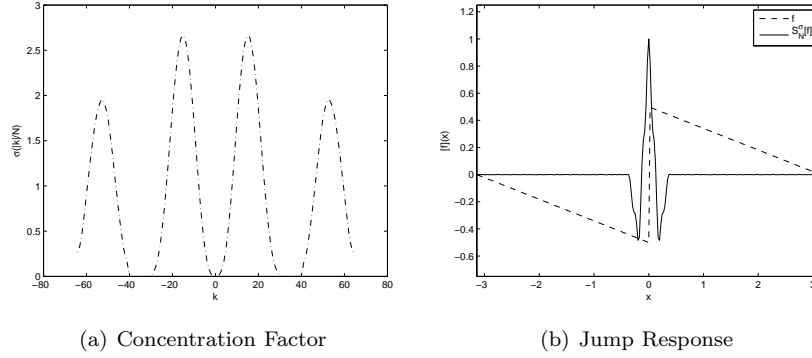0 & \text{else.}
\end{cases}
\tag{34}
$$

19

(a) Concentration Factor

(b) Jump Response

Figure 14: Concentration factor design for missing data, $N = 64$, modes $30 - 40$ missing.

(a) Jump Approximation – Problem Formulation 2

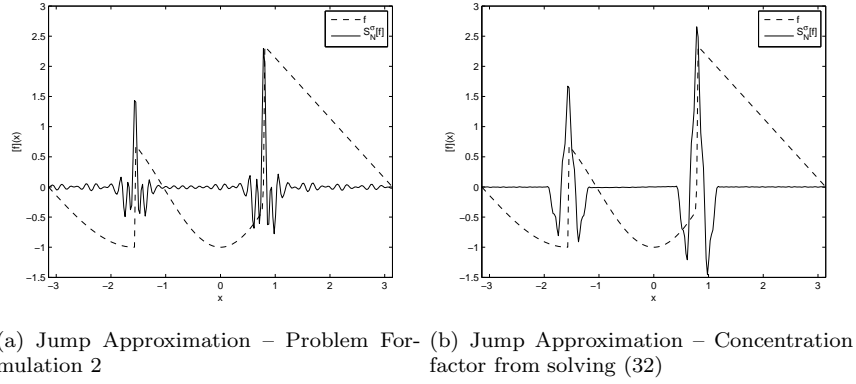(b) Jump Approximation – Concentration factor from solving (32)

Figure 15: Jump approximation of $f_3(x)$ from its Fourier modes, $N = 64$, modes $30 - 40$ missing.

The associated jump function is provided for reference in (34). As before, we note that the jump approximation is much cleaner. Moreover, with the standard concentration factors, the jump heights are not identified correctly. Recall (Section 2, admissibility conditions) that the concentration factors are required to satisfy a normalization constraint. This constraint is violated in the case of missing data, i.e., for the standard concentration factors

$$\sum_{\substack{k=1 \\ k \notin \mathbb{K}}}^{N} \frac{\sigma\left(\frac{|k|}{N}\right)}{k} < \sum_{k=1}^{N} \frac{\sigma\left(\frac{|k|}{N}\right)}{k} = 1. \tag{35}$$

Consequently, the jump response has the property that $W_0^{\sigma,N}(0) < 1$. This results in the jump height being incorrectly identified. It is only when the missing modes are explicitly modeled in the design process, the resulting concentration factor is suitably normalized, with

$$\sum_{\substack{k=1 \\ k \notin \mathbb{K}}}^{N} \frac{\sigma_{\text{mis}}\left(\frac{|k|}{N}\right)}{k} = 1. \tag{36}$$

5 Concluding Remarks

In this paper, we have introduced an iterative framework for the design of concentration factors for use in edge detection from Fourier data. Some of the traditional concentration factors have been shown to be obtained as specific formulations of the design framework. We have also demonstrated the use of this framework for the design of concentration factors from Fourier data missing a band of modes. Thus designed concentration factors have been shown to provide cleaner jump approximations, as well as more accurate jump values.

Some avenues for future investigation remain, including the incorporation of statistical characteristics of noise in the design process. The extension of this framework to the design of multidimensional concentration factors is also a problem of significant interest and importance.

References

[1] A. Gelb and E. Tadmor, *Detection of Edges in Spectral Data*, in Appl. Comp. Harmonic Anal., 7 (1999), pp. 101–135.

[2] A. Gelb and E. Tadmor, *Detection of Edges in Spectral Data II. Nonlinear Enhancement*, in SIAM J. Numer. Anal., Vol. 38, 4 (2000), pp. 1389–1408.

[3] A. Gelb, and E. Tadmor, *Adaptive Edge Detectors for Piecewise Smooth Data Based on the minmod Limiter*, in J. Sci. Comput., Vol. 28, 2–3 (2006), pp. 279–306.

[4] A. Gelb and D. M. Cates, *Detection of Edges in Spectral Data III– Refinement of the Concentration Method*, in J. Sci. Comput., Vol. 36, 1 (2008), pp. 1–43.

[5] S. Engelberg and E. Tadmor, *Recovery of Edges from Spectral Data with Noise–A New Perspective*, in SIAM J. Num. Anal., Vol. 46, 5 (2008), pp. 2620–2635.

[6] R. Archibald and A. Gelb, *Reducing the effects of noise in image reconstruction*, in J. Sci. Comp., Vol. 17, 1 (2002), pp. 167–180.

[7] E. Tadmor and J. Zou, *Novel edge detection methods for incomplete and noisy spectral data*, in J. Fourier Anal. Appl., Vol. 14, 5 (2008), pp. 744–763.

[8] E. Candes, J. Romberg and T. Tao, *Robust uncertainty principles: exact signal reconstruction from highly incomplete frequency information*, in IEEE Trans. Inf. Theory, Vol. 52 (2004), pp. 489–509.

[9] E. Candes, J. Romberg and T. Tao, *Stable signal recovery from incomplete and inaccurate measurements*, in Commun. Pure Appl. Math., Vol. 59 (2005), pp. 1207–1223.

[10] S.P. Boyd and L. Vandenberghe, *Convex optimization*, Cambridge Univ. Pr., (2004).

[11] M. Grant and S. Boyd, *CVX: Matlab software for disciplined convex programming (web page and software). http://stanford.edu/~boyd/cvx*, December 2008.

[12] M. Grant and S. Boyd, *Graph implementations for nonsmooth convex programs*, in Recent Advances in Learning and Control (a tribute to M. Vidyasagar), V. Blondel, S. Boyd, and H. Kimura, eds., Lecture Notes in Control and Information Sciences, Springer, 2008, pp. 95–110.

[13] K. S. Eckhoff, *Accurate and Efficient Reconstruction of Discontinuous Functions from Truncated Series Expansions*, in Math. Comp., Vol. 61, 204 (1993), pp. 745–763.